

Review

Charged particle multiplicity produced in neutrino-nucleon interactions at high energies

N. M. Hassan

Physics Department, Faculty of Science, Cairo University, 12613 Cairo, Egypt.

Accepted 27 April, 2007

The multi-particle productions in neutrino-nucleon collisions at high energy are investigated through the analysis of the data of the experiment CERN-WA-025 at neutrino energy less than 260 GeV and the experiments FNAL-616 and FNAL-701 at energy range 120-250 GeV. The general features of these experiments are used as base to build a hypothetical model that views the reaction through a Feynman diagram of two vertices. The first of which concerns the weak interaction between the neutrino and the quark constituents of the nucleon. At the second vertex, a strong color field is assumed to play the role of particle production, which depends on the momentum transferred from the first vertex. The wave functions of the nucleon constituent quarks are determined using the variation method and relevant boundary conditions are applied to calculation the deep inelastic cross sections of the virtual diagram.
PACS: 13.15. +g

Key words: Weak interaction, feynman diagrams, multiparticles.

INTRODUCTION

Observation of particles with large transverse momenta produced in high-energy collisions of hadrons and nuclei provides information about the properties of quark and gluon interactions. As follows from numerous studies in relativistic heavy ion physics (Satz, 1994; Laermann, 1996; Blaizot 1999) a common feature of the processes is the local character of the hadron interactions. This leads to a conclusion about dimensionless constituents participating in the collisions. On the other hand, the deep inelastic interactions of leptons with nuclei may reveal facts that relate the nature of particle production at lepton processes to that produced by hadrons. All these reasons had persuaded us to pursue the recent experiments of the neutrinos and antineutrinos with nucleons and nuclei to extract the general features of such collisions that enable to set up a relevant phenomenological model. The CERN experiment CERN-WA-025 (Tenner et al. 1992), and the Fermi National Lab experiments FNAL-616 (Oltman et al., 1992) and FNAL-701 (Aasratyan, 1993) are good samples to consider for examination. The first conclusion extracted from these experiments is the logarithmic relation between the average charged particle multiplicity and the lab energy of the incident neutrino as demonstrated by Figure 1. The figure shows also those

neutrinos (ν) produce more particles than antineutrinos ($\bar{\nu}$) at the same incident energy and in both cases the yield of particles is much less than the corresponding case of hadron nucleon collisions (Hussein et al., 1985). Moreover, Figure 2 shows that the values of the 2nd moment does not depend on the type of the projectile whether it is ν or $\bar{\nu}$ and this moment has the exponential form similar to that of hadron nucleon.

Finally, Figures 3 and 4 shows that F_2 and $x F_3$ are approximately independent on the momentum transfer square $|q^2|$, but instead depend on the Bjorken scalar scaling variable x . In this work, a hypothetical model is proposed assuming a Feynman diagram of two vertices. At the first one, the incident neutrino interacts with one of the nucleon constituent quarks by weak interaction and exchanges a heavy boson W or Z. The first vertex is considered as the source, which supplies the second vertex with energy that is used to create pairs of hadrons through strong interaction.

Of course, the charged and neutral currents due to W^\pm and Z^0 in this case have their own property that is responsible for different result of the hadrons. The paper is organized as follows: In section 2, we present the scenario of the model as well as the results and discussion. Brief

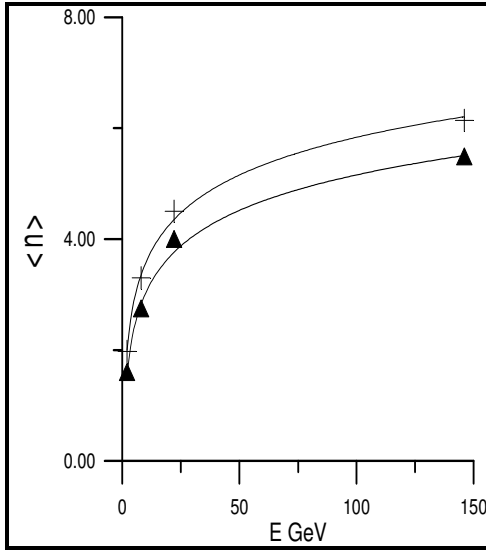


Figure 1. Average multiplicity of hadrons produced in π^- -D (black +) and D (\blacktriangle). The data concern the experiment CERN-WA-025. The solid lines are the parametric fitting curve with the form of for π^- -D, and for D experiment.

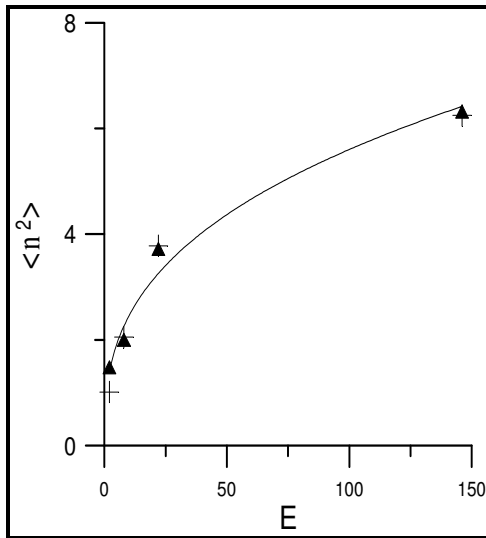


Figure 2. The second moment of the multiplicity of hadrons produced in π^- -D (black +) and D (\blacktriangle). The data concern the experiment CERN-WA-025. The solid line is the parametric fitting curve of the form.

summary and conclusive remarks are given in section 3.

A hypothetical model

The problem of multi particle production in ν -N collision is classified into two main parts. The first is to propose a relevant diagram to describe the process and specify the matrix element at its vertices. The second is to specify the wave function of the constituent particles of the tar-

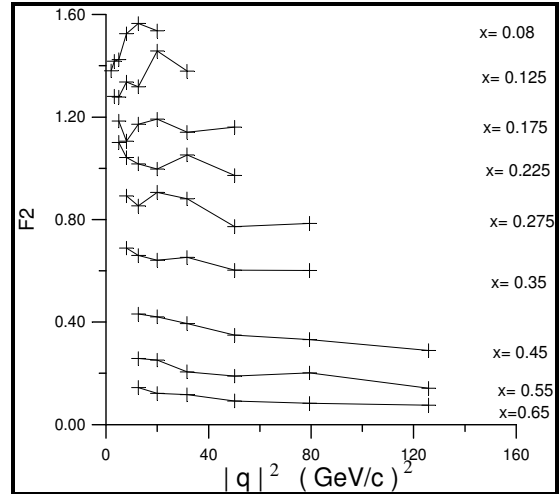


Figure 3. The structure function F_2 of the π^-p collision of the experiments FNAL-616 and FNAL-701 at energy range 120-250 GeV, with Bjorken scaling variable $0.08 < x < 0.65$.

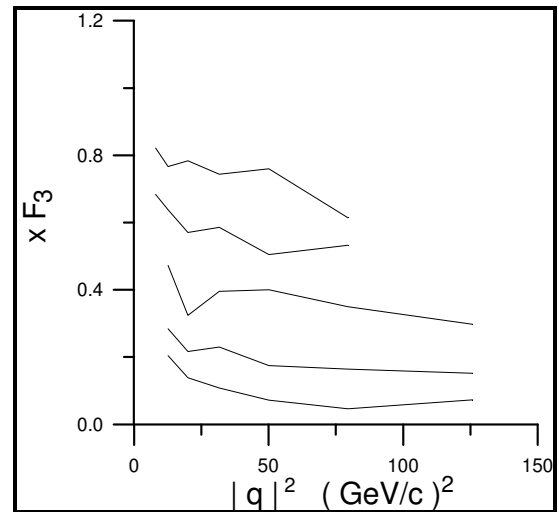


Figure 4. The structure function $x F_3$ of the π^-p collision of the experiments FNAL-616 and FNAL-701 at energy range 120-250 GeV, with Bjorken scaling variable $0.08 < x < 0.65$.

get. Our strategy is to use a Feynman diagram as shown in Figure 5 with two vertices. At the first, a weak interaction takes place and a strong interaction holds the second vertex. On the other hand, we follow the quantum variation method (Rajeev, 1991) to determine the parton wave function. Consider a two-dimensional Minkowski space, and we define the null momentum (Turgut and Rajeev, 1998) p as $p = p_0 - p_1$ where p_0 represents the total energy and p_1 is the longitudinal momentum, so that the mass shell condition for a particle of mass m : $p_0^2 = p_1^2 + m^2$ is replaced by the simple form;

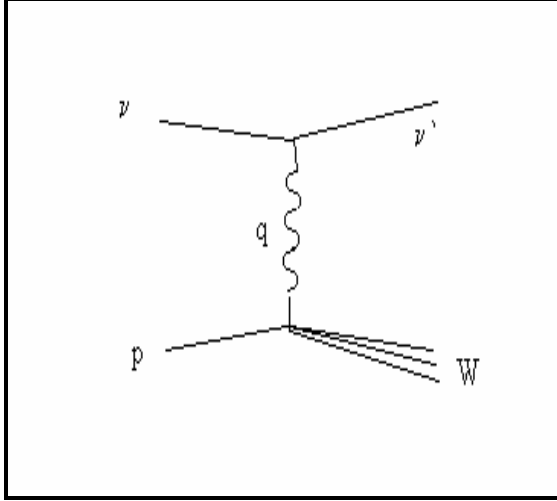


Figure 5. Feynman diagram describes the multiparticle production in \square -N collisions.

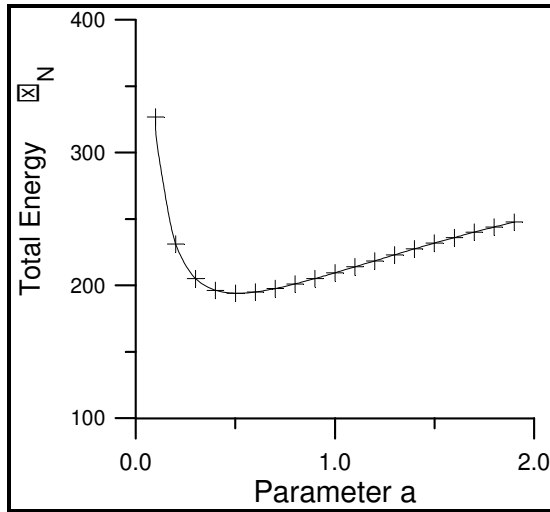


Figure 6. The variation of the total energy of the assembly of the quarks forming the nucleon shows that it has a minimum at a parameter value $a = 0.5$.

$p_o = \frac{1}{2} \left(p + \frac{m^2}{p} \right)$. In QCD, the force between quarks is

due to the exchange of gluons, which are massless bosons, and corresponds to the photons in QED. The long-range field between quarks may be considered as linear field in null coordinates and has a propagator $1/q^2$ in momentum space. Let us consider the nucleon as a relativistic quantum system of multi-particles. So that the nucleon is described in terms of wave function those depends on quantum numbers concerning the quarks (momentum, spin, color, flavors). The values of these parameters are determined to minimize the total energy of the

quark system of the nucleon (Figure 6). Since the quarks forming the nucleon have spin=1/2 and the nucleon is colorless, so it is convenient to write the parton wave function as $\tilde{\Psi}(a, \alpha, p)$, where a is the flavor (up or down), α is the color quantum number and p is the momentum in the null space. Then the nucleon wave function for N partons is $\tilde{\Psi}(a_1, \alpha_1, p_1; \dots; a_N, \alpha_N, p_N)$ and should be anti-symmetric under interchange of a pair of quarks, as the nucleons are Fermions. However, since the baryon is invariant under that of color, the wave function must be completely anti-symmetric in color alone.

$$\tilde{\Psi}(a_1, \alpha_1, p_1; \dots; a_N, \alpha_N, p_N) = \frac{\epsilon_{\alpha_1, \alpha_2, \dots, \alpha_N}}{\sqrt{N!}} \tilde{\Psi}(a_1, p_1; \dots; a_N, p_N) \quad (1)$$

The corresponding nucleon wave function in the position space $\{r_j\}$ is $\Psi(a_1, r_1; \dots; a_N, r_N)$ which is the Fourier transform of $\tilde{\Psi}(\{a_i, p_i\})$. If μ_a is the quark mass and the linear potential between a quark pair is $V(r_i - r_j) = \frac{g^2}{2} (r_i - r_j)$ where g^2 is the coupling constant, then the total energy of the nucleon is,

$$\xi_N = \sum_{a_1, \dots, a_N} \int_0^\infty \sum_{i=1}^N \frac{1}{2} \left(p_i + \frac{\mu_{a_i}^2}{p_i} \right) |\tilde{\Psi}(a_1, \dots, a_N, p_1, \dots, p_N)|^2 \frac{dp_1 \dots dp_N}{(2\pi)^N} \quad (2)$$

$$+ \frac{g^2}{2} \sum_{a_1, \dots, a_N} \int_{-\infty}^\infty \sum_{i \neq j}^N (r_i - r_j) |\Psi(a_1, \dots, a_N, r_1, \dots, r_N)|^2 dr_1 \dots dr_N$$

Starting with the simplest parametric form of the quark wave function,

$$\tilde{\Psi}_a(p) = C e^{-ap} \quad (3)$$

$$a > 0 \quad p \geq 0$$

And its Fourier transform is

$$\Psi(r) = \frac{C'}{(r + ia)^2} \quad (4)$$

Where C and C' are normalization constants, while a is a fitting parameter.

A more reasonable quark wave function with two variation parameters α and β may be written as,

$$\tilde{\Psi}(p) = C p^\alpha (1-p)^\beta \quad (5)$$

Again, inserting Equation 5 in Equation 2, this gives the total energy ξ_N of the quark assembly of the nucleon that shows multiple minima corresponding to different

Table 1. Eigen parameters of the parton states in the nucleon system.

Parton State	α	β	Energy (arbitrary unit)
E0	3.6	3.6	3.45E-6
E1	2.9	3.7	6.73E-6
E2	2.7	3.7	9.54E-6
E3	2.2	3.4	4.60E-5
E4	2.1	3.1	4.70E-4

energy levels whose eigen parameters α and β are listed in Table 1. The range of the null momentum p extends from zero up to P_{max} . It is more convenient to express the wave function and all other physical quantities in terms of the Bjorken scaling variable $x = p/P_{max}$ with x lies in the range ($0 < x < 1$)

The ground state E0 has equal values in the parameters α and β which means that the state has line symmetry about $x=0.5$, in other words, the probability that a parton has a value x is equal to that of $(1-x)$. The symmetry breaks at the higher-up states, where the probability increases towards the deep inelastic $x < 0.5$.

The total scattering amplitude due to the diagram Figure 5 is written as:

$$\Gamma_{tot} = \prod_i \Gamma_i = \prod_i \langle \psi_i | G_i | \psi_i \rangle \quad (6)$$

Where Γ_i is the scattering amplitude at the i^{th} vertex of the diagram, and G_i is the relevant propagator. At the first vertex, where a weak interaction holds, we used a plane wave for the neutrino wave function and a weak propagator of the form, $1/(q^2 + M_{w,z}^2)$, where $M_{w,z}^2$ represents the mass of the exchange Boson (Abreu et al., 2000). While strong field acts at the second vertex, associated with an exponential form factor, so that Γ_{tot} could be written as,

$$\Gamma_{tot}(x, q^2) = \frac{1}{q^2 + M_{w,z}^2} \text{Exp}(-\gamma q^2) |\tilde{\Psi}(x)|^2 \quad (7)$$

$\tilde{\Psi}(x)$ is the quark wave function defined by Equation 3 and 5. The problem of particle production is to be viewed through the relativistic phase space. Following the scheme of Ref. (Hussein and Cimento 1993) (see appendix A), it is easy to define the cross section of finding n -particles in the final state with total center of finding n -particles in the final state with total center of mass energy $\sqrt{s} = W$, $W^2 = (p_a + p_b)^2$

$$\sigma_n = \frac{1}{F} \int \dots \int \prod_i \left\{ \frac{d^3 p_i}{2E_i} \right\} \delta^4(p_W - \sum p_i) |\Gamma(p_i)|^2 \quad (8)$$

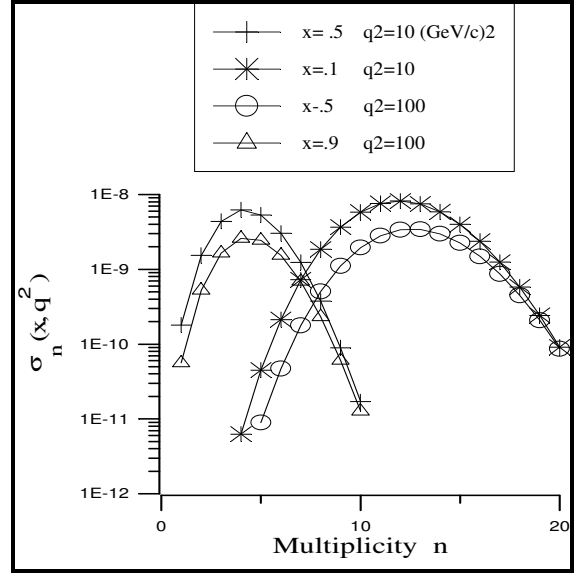


Figure 7. The multiplicity distribution of charged secondaries in p collision as a function of both x and q^2

Where F represents the incident flux, p_w and p_i being the four-vector momentum carried by the propagator W and the created hadrons respectively. The delta function is to conserve the four-vector momentum at the 2nd vertex of the reaction. It also restricts the integration over a surface of $3n-4$ dimensional space. The multi-dimensional integration in Equation 8 may be solved using the Monte Carlo technique. However the volume of such n -dimensional sphere may be approximated at extremely high energy as,

$$\sigma_n = \frac{1}{F} \frac{(\pi/2)^{n-1}}{(n-1)!(n-2)!} W^{2n-4} |\Gamma(p)|^2 \quad (9)$$

Transforming Equation 8 from the momentum space to the Bjorken scaling variable x and writing the energy W in terms of the kinematical variables of diagram (5)

$$W^2 = m^2 + q^2 \left(\frac{1}{x} - 1 \right), \text{ then}$$

$$\sigma_n(x, q^2) = \frac{1}{F} \frac{(\pi/2)^{n-1}}{(n-1)!(n-2)!} [m^2 + q^2 \left(\frac{1}{x} - 1 \right)]^{n-2} |\Gamma(x, q^2)|^2 \quad (10)$$

The implementation of Equation 10 leads to the formation of Figure 7, which shows that the cross section of production of n -particles depends appreciably on x and weakly on q^2 . The decrease of x means going towards the deep inelastic, which offer more fraction of energy for creation of particles and this increases the peak of the multiplicity towards higher values. The overall multiplicity distribution is found by integrating over x from 0 to 1 and

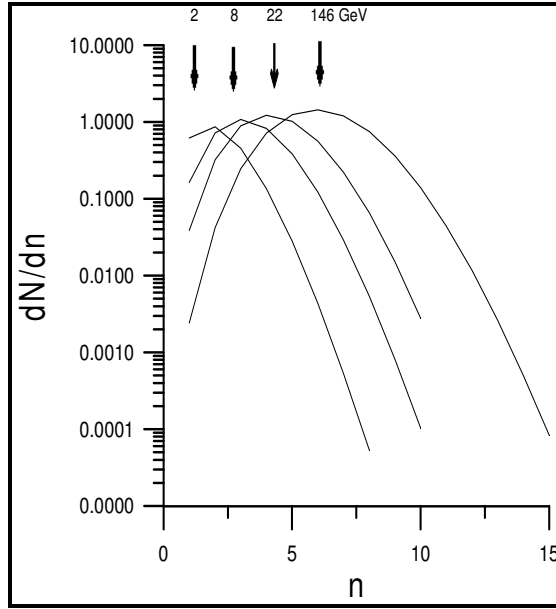


Figure 8. The overall multiplicity distribution of charged secondaries produced in νp collision at ν -energies of 2, 8, 22 and 146 GeV as predicted by the model.

Table 2. The average multiplicity $\langle n \rangle_{th}$ of hadrons produced in ν -nucleon collisions as predicted by the model using the one parameter parton wave function compared with the experimental data.

Cut off	$E\nu$	Γ	$\langle n \rangle_{ex}$	$\langle n \rangle_{th}$
0.075	2	0.5	1.97	2.1
0.070	8	0.5	3.30	3.31
0.020	22	0.5	4.50	4.35
0.001	146	0.5	6.14	6.17

over q^2 from q_{min}^2 to q_{max}^2 . A cutoff value of q^2 is necessary to keep the system in the physical region of the phase space. The cutoff ratio is taken as a free parameter in this model to fit the experimental data. The multiplicity distributions of secondary hadrons are demonstrated in Figure 8 for ν -energies of 2, 8, 22 and 146 GeV, the average values of each are listed in Table (2) with the considered parameters. The comparison with the experimental data shows very good agreement. The cross section $\sigma_n(x, q^2)$ is recalculated again using the parton wave function as given in Equation 5 for the first 3-parton states only E0, E1 and E2 with the corresponding parameters as in Table (1). The results are given in Table (3) for the average multiplicity compared with the experimental values that show also good agreement. In fact the comparison with the average value of the multiplicity is not enough to reflect the validity of a hypothetical model; nevertheless, it may indicate that the work is going in the right way. The calculation of the

differential cross section $d^2\sigma/dx dq^2$ may give more information on such reactions. The increase of the yield in ν -N collisions than the case of $\bar{\nu}$ -N may be explained by taking into account the leptonic weak current, which depends mainly on the proposed hypothetical neutrino (anti-neutrino) wave function.

Summary and conclusive remarks

1. The average multiplicity of hadrons produced in ν -nucleon interactions have a logarithmic dependence on the energy of the incident neutrino. The yield in ν -N is slightly greater than the corresponding figure in $\bar{\nu}$ -N.
2. The Feynman diagram with two vertices may successfully describe the ν -N interaction. A weak interaction holds at the first vertex and a strong interaction works at the second one where hadrons are created. W and Z bosons are assumed as the exchange particles in the weak interaction.
3. The first vertex of the Feynman diagram is assumed as the source, which supplies the energy to the second vertex. That energy is responsible for hadron creation. The rate of energy transfer is controlled by the matrix element of weak interaction at the first vertex.
4. The average multiplicity of produced hadrons is strongly dependent on the Bjorken scaling variable x and weakly on the momentum transfer q^2 .

Appendix A

The multi-peripheral technique

In this technique, the many body-systems is expanded into subsystems, each concerns a two body collision. It is assumed that each hadron in the final state is produced at a specific peripheral surface that is characterized by a peripheral parameter. The phase space integral $I_n(s)$ of the produced hadrons is a measure of the probability of producing n particle in the final state at center of mass energy $W=\sqrt{s}$. It depends mainly on the volume in phase space and the transition matrix element T , and defined as,

$$I_n(s) = \int \dots \int \prod_i^n \frac{d^3 p_i}{2E_i} \delta^4(s - \sum_j p_j) |T|^2 \quad (A-1)$$

Equation (A-1) may be simplified as if expressed as a sequence of two-particle decay. Accordingly, the integration in Equation (A-1) becomes,

$$\begin{aligned} I_n(s) &= \int_{\mu_{n-1}^2}^{(M_n - m_n)^2} dM_{n-1}^2 I_2(k_n^2, k_{n-1}^2, p_n^2) I_{n-1}(M_{n-1}^2) |T|^2 \\ &= \int_{\mu_{n-1}^2}^{(M_n - m_n)^2} dM_{n-1}^2 \int d\Omega_{n-1} \frac{\lambda^{1/2}(M_n^2, M_{n-1}^2, m_n^2)}{8M_n^2} I_{n-1}(M_{n-1}^2) |T|^2 \end{aligned} \quad (A-2)$$

Table 3 The average multiplicity $\langle n \rangle_{th}$ of hadrons produced in ν -nucleon collisions as predicted by the model using the two parameter parton wave function, at the first three energy levels compared with the experimental data.

E0		E1		E2		$\langle n \rangle_{ex}$	E_ν
$\langle n \rangle_{th}$	γ	$\langle n \rangle_{th}$	γ	$\langle n \rangle_{th}$	γ		
2.10	1.0	2.15	1.1	2.23	1.15	1.97	2
3.31	0.31	3.32	.36	3.5	.37	3.3	8
4.35	0.20	4.41	.26	4.51	.27	4.5	22
6.17	0.03	6.16	.033	6.14	.033	6.14	146

The integration over all possible values of M_{n-1} concerns the first vertex in the chain. To proceed further, we iterate Equation (A-2) for the M_{n-2} , M_{n-3} , ..., M_2 to obtain the entire chain, so that,

$$I_n(s) = \int_{\mu_{n-1}}^{(M_n - m_n)} dM_{n-1} d\Omega_{n-1} \frac{1}{2} P_n |T(p_{n-1})|^2 \cdots \int_{\mu_2}^{(M_3 - m_3)} dM_2 d\Omega_2 \frac{1}{2} P_3 |T(p_2)|^2 \cdot \int d\Omega_1 \frac{1}{2} P_2 |T(p_1)|^2 \quad (A-3)$$

Where

$$P_i = [(M_i^2 - M_{i-1}^2 - m_i^2)^2 - 4M_{i-1}^2 m_i^2]^{1/2} / 2M_i \text{ is}$$

The three-vector momentum of the i^{th} particle and $T(p_i)$ is the transition matrix element at the i^{th} peripheral surface. For the case of strong interactions $T(p_i)$ has a parametric form as,

$$T(p_i) = \exp(-\alpha_i p_i) \quad (A-4)$$

And α_i is a peripheral parameter, which fits the experimental data. The multiple integration in Equation (A-3) may be solved by the Monte Carlo technique. At extremely high energy, Equation (A-3) has an asymptotic limit in the form;

$$I_n(s) = \frac{(\pi/2)^{n-1}}{(n-1)!(n-2)!} s^{n-2} |T|^{2(n-1)} \quad (A-5)$$

REFERENCES

- Satz H (1994). The evolution of the Quark-Gluon plasma. Nucl. Phys. A566: 1c.
- Laermann E (1996). Recent results from lattice QCD simulations. Nucl. Phys. A610: 1c.
- Weise W (1999). QCD aspects of hadron physics, Nucl. Phys. A661: 3c.
- Hassan NM (2006). Neutrino-Nucleon Interaction through intermediate vector Boson Fizika B15: 37
- Tenner AG (1994). Slow proton production in deep-inelastic neutrino scattering on deuterium, Phys. Rev. C49: 2379
- Blair IM (2002). Upper limits for neutrino oscillations muon-antineutrino to electron-antineutrino from muon decay at rest, Phys.Rev. D65, 112001
- Aasratyan AE (1993). Diffractive production of charmed strange mesons by neutrinos and antineutrinos, Z. Phys. C58: 55
- Hussein MT (1985). Multiparticle production in proton-proton collisions at high-energies. Canad. J. Phys. 63:1449.
- Rajeev SG (1991). Lecture in Summer School in High Energy and cosmology Vol II, ICTP, Trieste, Italy.
- Teoman Turgut O (2003). On two dimensional coupled bosons and fermions. J. Math. Phys. 44: 198.
- Abreu P (2000). (DELPHI Collaboration), Measurement of the B/s0 Lifetime and Study of B/s0 anti-B/s0 Oscillations using D/s I Events Eur. Phys. J. C18: 203.
- Hegab MK, Hussein MT, Hassan NM (1990). Nucleus-Nucleus Collisions at High Energies. Z. Phys. A 336: 345
- Hussein MT (1993). Hadron -Nucleon Interactions in View of a Multi-peripheral Model., IL Nuovo Cimento 106 A: 481.